Progress In Electromagnetics Research, PIER 91, 229–242, 2009

DEVELOPMENT AND ELECTROMAGNETIC CHARACTERIZATION OF ADAPTABLE OPEN-ARCHITECTURE WLAN SYSTEMS

V. P. Papantoniou and T. D. Xenos

Department of Electrical and Computer Engineering
Aristotle University of Thessaloniki
Thessaloniki 54124, Greece

Abstract—The construction and comprehensive electromagnetic analysis of a novel class of WLAN layouts is presented in this paper. The main purpose is to construct a wireless system according to the 802.11 a/b/g standards, which enables significantly larger and more reliable data transfer rates, making use of a new large-scale field prediction technique, based on the parabolic equation with finite differences. Thus, four distinct structures, based on two different operating systems and two different hardware architectures, are proposed and elaborately examined. On the other hand, for the prediction algorithm a 3D wide-angle parabolic equation scheme is devised and a recursive approximation of the forward wave equation is accomplished. Unlike existing methods that characterize obstacles by means of surface impedance boundary conditions, a more rigorous approach, by treating them as penetrable objects with known material features is utilized. In this manner, the "interface" problem is systematically formulated and high levels of accuracy are attained. Moreover, the proposed technique is proven to be sufficiently faster and numerically more efficient, as the lattice, so constructed, along with the numbering of degrees of freedom remain unchanged from a parabolic equation plane to another. Extensive results and measurements certify the aforementioned merits for various realistic exterior and interior configurations.

Corresponding author: V. P. Papantoniou (bpap@ee.auth.gr).

1. INTRODUCTION

The technological advancements in the field of wireless local area networks (WLANs) have recently gained a tremendous growth and the design of efficient, economical, and reliable models is an issue of paramount importance and intense research. Actually, the correct realization of a WLAN is an outgrowth of several closely related factors [1, 2]. Towards the process of an efficient network planning, the development of efficient computational techniques for the characterization of propagation in modern wireless communication scenarios is of great importance, since the precise positions of the transmitters and receivers needs to be determined to maximize network performance, security and compliance with safety regulations. The basic methodologies for this purpose belong to the general category of ray-tracing techniques [3–6] and their correct application has a significant impact on the design of modern WLAN antennas [7–21]. Such methods incorporate simplified models of electromagnetic wave reflection, refraction and diffraction and require a large number of rays to be considered for an acceptable propagation analysis. In the case of a metropolitan area network, the situation becomes more complex, since two different propagation settings should be treated at the same time. The first one is the urban propagation problem, since two network nodes can be at distances of up to several hundreds of meters and the buildings can cause significant attenuation of the signal, as long as serious multipath effects and fading. On the other hand, access points in a wireless metropolitan network are not necessarily placed on rooftops, towers or other elevated structures. In case they are placed near windows, the "interface" problem of urban-to-indoor propagation should be considered as well. The alternative solution seems to be the introduction of parabolic equation (PE) methods [22–25], since the propagation takes place largely around a main axis but its application to urban wave propagation is restricted in simple models.

It is the aim of this paper to develop a novel family of adaptive Wi-Fi systems, based on modern open-architectures with enhanced performance and user-friendly features. In this context, four alternative platforms, based on two different operating systems (Linux and FreeBsd) and two different hardware architectures, have been developed and thoroughly investigated. The first architecture is founded on the aspects of embedded technology/single-board network processor, while the second one uses the industrial Mini-ITX motherboards in X86 architecture. Except for the in vitro examination, particular attention is drawn to the simulation of a real-world traffic burden via interactive software as well as the elaborate analysis of all

possible upgrade costs. The analysis here will be performed via a 3D wide-angle parabolic equation (PE) method, based on a finite difference implementation and a recursive approximation of the forward wave equation. Unlike present approaches that characterize buildings and obstacles via surface impedance boundary conditions, we attempt here a more rigorous approach by treating them as penetrable structures with known material characteristics. This technique has three obvious advantages: First, it will efficiently deal with the "interface" problem, since the exact configuration of the nearby walls, window panes and other surrounding penetrable structures near the access points will be accurately modeled. Second, although for other structures in the main urban wave propagation path (other buildings, metallic structures etc.) it is not essential to compute the field inside them, it is expected that such a treatment will be more accurate, since the surface impedance approximation is not correct, particularly for materials of low conductivity. Finally, the proposed approach has the additional advantage of being fast and numerically efficient, since the FD grid, numbering of degrees of freedom etc. are identical from a PE plane to another. The necessary preprocessing is also done once, at the beginning of the marching-in-space procedure, while most of the system matrix entries can be also computed beforehand.

The full 3D solver that has been developed is successfully applied to realistic propagation problems within domains that span hundreds or even thousands of wavelenghts in length and several thousands of square wavelengths in cross-section and is made highly automated, taking data extracted from digital maps and other GIS databases. Most importantly, the electromagnetic analysis will provide optimal configurations of the transmitting and receiving antennas, in terms of precise location, direction angle etc., that can be exploited to maximize throughput and efficiency of the network.

2. DESCRIPTION OF THE NEW WIRELESS SYSTEMS

The first wireless configuration is based on the embedded technology/single-board network processor. Actually, this is a stand-alone computational system which uses a low consumption processor. Moreover, it has a full network support and on-board mini-PCI adapters, intended for the implementation of the wireless access point, bridge or client. The proposed platform also enables operation frequencies at 2.4 and 5 GHz via the appropriate mini-PCI wireless cards at the corresponding frequency spectra. Among its most prominent merits is its modular nature that allows easy and rapid incorporation to already existing antenna structures, and its low power requirements

(a maximum of 12 W).

On the other hand, the second arrangement utilizes Mini-ITX motherboards based on the X86 architecture. For this purpose, full computer systems are installed which, despite their small dimensions, provide all the main features of a typical PC, basically regarding computational competences and network traits. Again, the existence of Mini-PCI adapters leads to its efficient realization as an access point/bridge/client. As for the choice of operation system, several Linux and FreeBsd versions have been installed and tested.

To validate the performance of the aforementioned structures in the laboratory, two regular PCs have been utilized. After the necessary stability and transfer-rate tests, the whole implementation was established in a couple of Mini-ITX industrial boards. In all measurement setups inside the laboratory, the distance between the two points varied from 5 to 20 meters. In contrast at external regions, two different topologies were used: (a) a 2.5 km point-to-point link at 2.4 and 5.76 GHz and (b) a 6.5 km multi-point link at 5.76 and 5.8 GHz. As for the electromagnetic characterization of all configurations, a user-friendly and interactive software, necessary to complement the measurement process, is developed, as described in the next section. Several features are analyzed to get the best knowledge on the behavior and the advantages or weaknesses of the arrangements. Also, the influence of all fading mechanisms is carefully studied for diverse propagation models and operational parameters.

3. THE 3D WIDE ANGLE PE-FD METHOD

The estimation of received power is performed by a thorough computational analysis based on the parabolic equation. This results from the assumption that the directions of propagation are close to a primary axis (e.g., the x-axis) and, hence, the variation of the electric field is decomposed in a rapid phase variation along the main direction and a wave-envelope that exhibits much smoother spatial variations, i.e.,

$$\mathbf{E}(x, y, z) = \tilde{\mathbf{E}}(x, y, z)e^{-jk_{ref}x}, \tag{1}$$

where $k_{ref} = k_0 n_{ref}$ is the reference wavenumber, (e.g., the free-space wavenumber k_0 for propagation in free space). By substituting (1) in Helmholtz equation and retaining second order variations of the wave-envelope, the wide-angle PE

$$\frac{\partial \tilde{\mathbf{E}}}{\partial x} - j\frac{1}{2k_{ref}}\frac{\partial^2 \tilde{\mathbf{E}}}{\partial x^2} = j\frac{1}{2k_{ref}}P\tilde{\mathbf{E}}(x, y, z), \tag{2}$$

is derived, where the transverse differential operator is

$$P \equiv k_0^2 \left(n^2 - n_{ref}^2\right) + \nabla_t^2. \tag{3}$$

However, for an efficient marching-in-space implementation of (2), only the first derivative should be present. If the second derivative is considered negligible, we get the paraxial approximation, which is valid for small angles, usually up to 7 degrees with respect to the main axis. To extend the validity of the PE, we rewrite the first-order differential operator in (2) in the recursive form

$$\frac{\partial}{\partial x} = \frac{j\dfrac{1}{2k_{ref}}P}{1 - j\dfrac{1}{2k_{ref}}\dfrac{\partial}{\partial x}}, \tag{4}$$

which can be successively applied again in (2) to come up with the first order correction

$$\left\{-j2k_{ref} - j\frac{1}{2k_{ref}}\left[\nabla_t^2 + k_0^2\left(n^2 - n_{ref}^2\right)\right]\right\}\frac{\partial\tilde{\mathbf{E}}}{\partial x} = -\left[\nabla_t^2 + k_0^2\left(n^2 - n_{ref}^2\right)\right]\tilde{\mathbf{E}}. \tag{5}$$

For most scenarios of urban wave propagation, it turns out that this correction is enough to account for most important propagation rays and the second correction does not offer a significant improvement. The discrete form of (5) results if we relate the wave-envelope values at the transverse plane $p+1$ to those at plane p, by discretizing (5) along the propagation axis, using the Crank-Nicholson method

$$\left\{-j2k_{ref} - j\frac{1}{2k_{ref}}P\right\}\frac{\tilde{\mathbf{E}}^{p+1} - \tilde{\mathbf{E}}^{p}}{\Delta x} = -P\left[a\tilde{\mathbf{E}}^{p+1} + (1-a)\tilde{\mathbf{E}}^{p}\right]. \tag{6}$$

It can be easily proved that (6) corresponds to a formulation similar to the paraxial parabolic equation, i.e., (2), without the second order derivative, where the usual Crank-Nicholson parameter $a \geq 1/2$ is simply replaced by

$$a_{WA} = a + \frac{1}{j2k_0\Delta x}. \tag{7}$$

This modification is enough to correctly model propagation angles up to 15–20 degrees from the axis and is sufficient for all cases considered here, as demonstrated in the numerical examples.

Finally, the termination of the open space is performed by the uniaxial perfectly matched layer (PML) [26]. The transverse laplacian

in Helmholtz equation, is modified as

$$\frac{\partial^2 \tilde{\mathbf{E}}}{\partial x^2} + \frac{1}{s_y}\frac{\partial}{\partial y}\frac{1}{s_y}\frac{\partial \tilde{\mathbf{E}}}{\partial y} + \frac{1}{s_z}\frac{\partial}{\partial z}\frac{1}{s_z}\frac{\partial \tilde{\mathbf{E}}}{\partial z} + k_0^2 \varepsilon_r \tilde{\mathbf{E}} = 0, \tag{8}$$

where s_y, s_z are the PML parameters, given by

$$s_y = 1 - j \tan\delta \left(\frac{y}{d}\right)^2, \quad \tan\delta = \frac{3\lambda}{4\pi d} \ln\frac{1}{R}, \tag{9}$$

where d is the PML width, y the distance from the air-PML interface and R the desired reflection coefficient. Equations (4)–(9) are still valid, with the only modification being in the form of the transverse differential operator

$$P = k_0^2 \left(n^2 - n_{ref}^2\right) + \frac{1}{s_y}\frac{\partial}{\partial y}\frac{1}{s_y}\frac{\partial}{\partial y} + \frac{1}{s_z}\frac{\partial}{\partial z}\frac{1}{s_z}\frac{\partial}{\partial z}. \tag{10}$$

Discretization of (6) and (10) is performed by central finite differences, resulting in a sparse system of the form

$$\mathbf{A}\underline{\tilde{\mathbf{E}}}^{p+1} = \mathbf{B}\underline{\tilde{\mathbf{E}}}^{p}, \tag{11}$$

where $\underline{\tilde{\mathbf{E}}}^{p+1}$, $\underline{\tilde{\mathbf{E}}}^{p}$ are column vectors of the wave-envelope values at the corresponding steps. The system matrix is well-conditioned and each system is solved quite fast, using the biconjugate gradient stabilized technique. A considerable convergence improvement is attained by using the lower triangular part of the system matrix as a preconditioner.

We stress the fact that thanks to the modeling of obstacles as penetrable materials, the FD matrix formation is done basically once. The changing part of the matrix, due to the change of structures and materials is in the form of a diagonal matrix, which is updated in each PE step in a very fast manner. The only issue that needs to be addressed in the PE method, where different materials are present in the structure, is the careful choice of the reference refractive index and the use of slightly finer discretization, which is necessary for dealing with wide propagation angles anyway. For high contrast scatterers, a reference index equal to the mean values of the various material indices seems to work well in all cases.

4. COMPUTATIONAL RESULTS

Before the application of the proposed method to real world large-scale propagation problems, a validation through comparisons with

problems that admit an analytical solution is attempted. First, the propagation of a Gaussian beam in free space is studied, to assess the accuracy and applicability of the method to problems spanning hundreds or thousands of wavelengths. The comparisons for propagation distances of 500 and 5000 wavelengths are shown in Fig. 1, both for a transverse computational window of 100 $\times$ 50 square wavelengths. The Gaussian beam at the initial plane has an amplitude equal to one and a spot size equal to twice the wavelength. The resolution in the transverse plane is equal to a quarter wavelength, while the step size of the parabolic equation technique is half wavelength. The number of PML layers was set to 24, while the theoretical PML reflection coefficient in (9) was set to a very low value of 1e-96. Such a low value is considered essential, since for

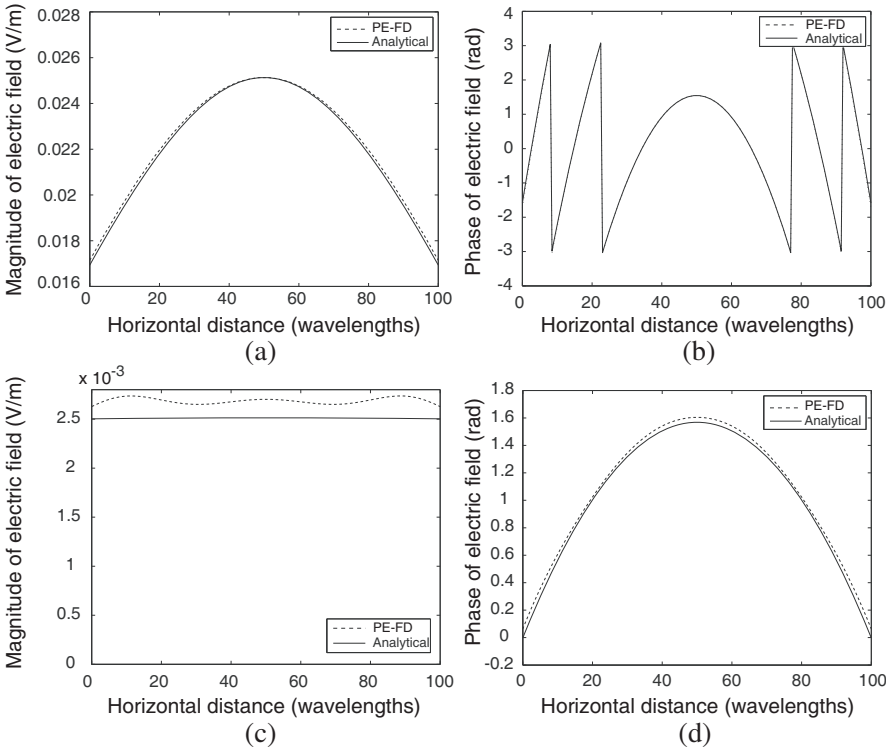

Figure 1. Comparison of PE-FD method to the analytical solution for a Gaussian beam: (a) magnitude and (b) phase for a 500 wavelength propagation distance; (c) magnitude and (d) phase for a 5000 wavelength propagation distance.

long propagation distances, grazing incidence dominates, necessitating a very high absorption. The agreement of results is excellent, even in the case of a very large propagation distance, with a maximum deviation of 0.5 dB. Next, the more challenging problem of scattering from a conducting cylinder of diameter equal to 10 wavelengths is considered. The field is computed along a line transverse to the direction of propagation and at 10 wavelenghts from its center, with a vertically polarized plane wave as an excitation. The computational window is 20×80 square wavelengths, while the transverse resolution and step size are a quarter and half wavelength, respectively. The PML settings are the same as before. The electric field behind the scatterer is compared to the analytical solution (Fig. 2). The results are in very good agreement as well.

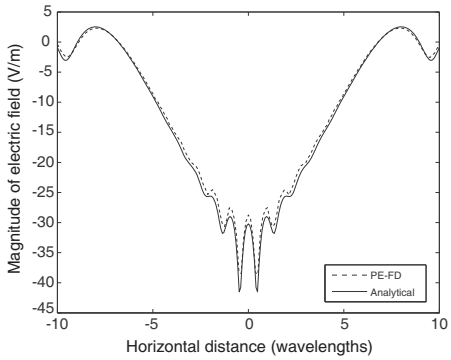

Figure 2. Magnitude of electric field behind a conducting cylinder of diameter equal to 10 wavelengths, along a line transverse to the direction of propagation and at 10 wavelenghts from its center.

The next step is the realistic application in a long-distance metropolitan area network link. The geometry of the experimental link that has been set up is shown in Fig. 3. Using, the proposed method, an accurate field prediction is possible, regardless of the antenna positions. The measured received power has been shown to agree with the computed one with a margin of ± 5 dB in all cases. Most importantly, the optimal positions to place the user antenna can be predicted. Such points of higher received power due to positive superposition of diffracted fields can be exploited for increased performance. Graphs of the electric field along a transverse line are shown in Figs. 4(a) and 4(b), for the frequencies of 2.4 GHz and 5.76 GHz, respectively. The solutions have been obtained by successively solving linear systems of 84744 and 356460 degrees of freedom, respectively. The simulations

Figure 3. Experimental link between the School of Engineering, Aristotle University of Thessaloniki and the receiving site. The distance is about 2500 meters.

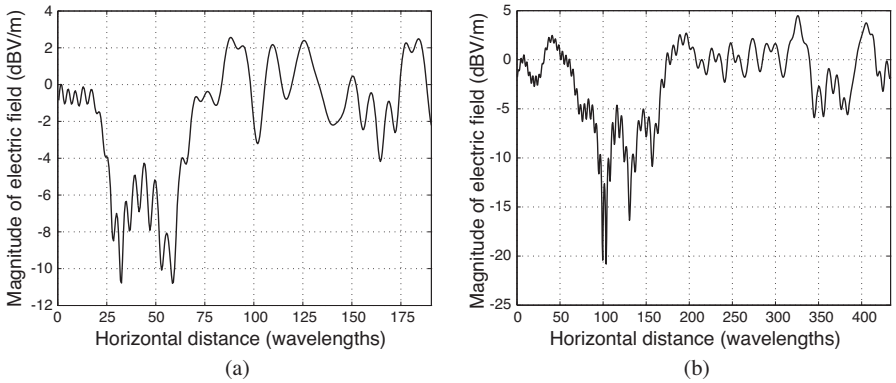

Figure 4. Normalized electric field along a line transverse to the direction of propagation for 2.4 GHz (a) and 5.76 GHz (b). The effect of two adjacent buildings is shown as a reduction of the field magnitude, while at several points the field is significantly raised due to a positive superposition of the diffracted field.

were completed in less than half an hour in the first case and about four hours in the second case, both in a high-end PC. In particular, the time-averaged deviations between the measured signal and the simulation, at the optimal position where the antenna mast has been installed, were found to be +4.23 dB and −2.50 dB, for the 2.4 GHz and 5.76 GHz links, respectively.

It is obvious that the user antenna can and should be placed at a

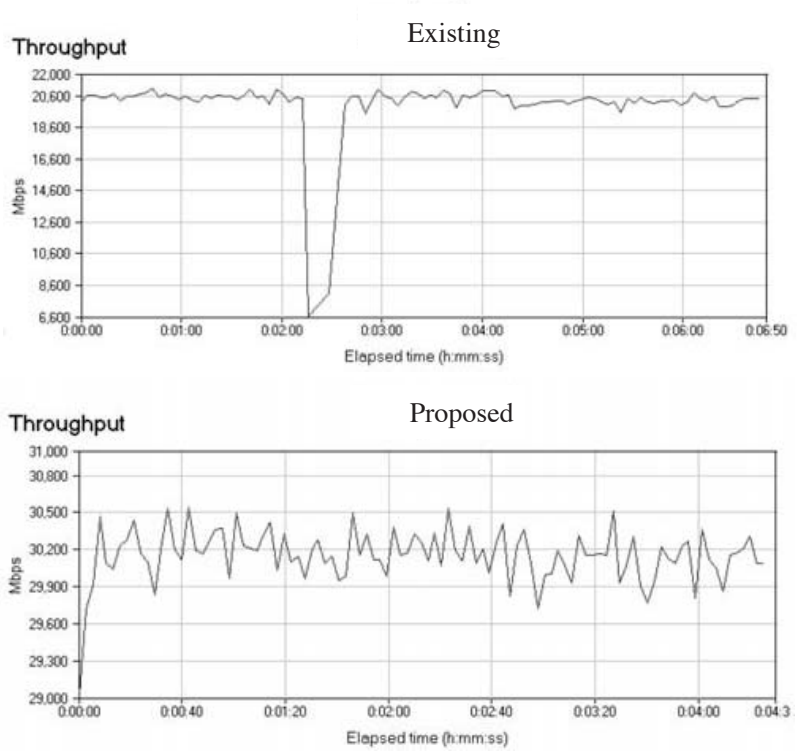

Figure 5. Performance enhancement via measured throughput, using the open architecture, in conjunction with the application of the proposed accurate field prediction technique.

position of a maximum. However, it is highly unlikely that this precise location can be found by measurements, since there are not only two degrees of freedom involved (height and horizontal displacement) but also these locations are high above the rooftop of the building and are practically inaccessible for measurements. In addition, there is a possibility that a random placement of the antenna will be detrimental to the received signal power, which is the case of the local minimum at the location of approximately 100 wavelengths, indicated in Fig. 4(a). Therefore, the position to install the antenna's supporting tower has to be wisely chosen. Another very interesting observation is that the optimal position can be at a horizontal displacement that is quite far from the direct line of sight, i.e., the center of the computational window (which is the case in Fig. 4(b), showing a maximum at a horizontal position of approximately 325 wavelengths). In such a

Table 1. Features and comparative results of the proposed WLANs.

WLAN Band	Implementation	Data Rate (Mbit)	Upgradability	Network Routing Capabilities
802.11 b/g [3]	Existing	18–20	Limited	Minimal
	Proposed	25–35	Full-open Architecture	Advanced
802.11 a [1, 2]	Existing	25	Limited	Minimal
	Proposed	70	Full-open Architecture	Advanced

case, the optimal location can be moved in a position that is more favorable to install the antenna's supporting tower, by slightly rotating the transmitting antenna.

Using the guidelines provided by the electromagnetic analysis, the antennas have been properly installed at optimal positions and angles. A characteristic graph of the measured overall improvement in network performance (throughput), using the combined open architecture and electromagnetic field prediction techniques are shown in Fig. 5, while mean performance values and other basic characteristics of the two protocols used are shown in Table 1.

5. CONCLUSION

In this paper, a family of efficient WLAN structures with two different operating systems and two different hardware architectures, have been introduced and studied in terms of design parameter optimality and performance. Furthermore, a prediction methodology featuring a 3D wide-angle parabolic equation scheme has been proposed in accordance with the new systems. Contrary to conventional approaches that characterize obstacles by means of surface impedance boundary conditions, a more precise realization by treating them as penetrable objects is employed. Hence, the hard "interface" problem is carefully manipulated in faster and more accurate sense. The proposed combination of the novel wireless configurations and the PE-FD technique for field prediction was proven to provide very fast and reliable network performance. The computational method offers accurate estimates of the received power and even predictions of optimal antenna locations. Comparisons with existing systems show that for transfer rates up to 25 Mbps, the embedded technology

concept exhibits a sufficient performance, although speeds in the level of 50 Mbps could be marginally at hand. However, the actual difference is spotted in the X86 architecture, where transfer rates up to 70 Mbps were attainable. Finally, the use of proprietary (non standard) protocols leads to speeds that reached 90 Mbps. The implementation is performed by applying firm and specific design principles, thus extracting the maximum performance, from both the nonstandard implementation and the field prediction technique.

REFERENCES

1. "Wireless MAC and PHY specifications: High speed physical layer in the 5 GHz band," IEEE 802.11a/D7.0, 1999.
2. "Wireless MAC and PHY specifications: Further higher-speed physical layer extension in the 2.4 GHz band," IEEE 802.11g, 2003.
3. Catedra, M. F., J. Perez, F. Saez de Adana, and O. Gutierrez, "Efficient ray-tracing techniques for 3D analyses of propagation in mobile communications: Application to picocell and microcell scenarios," *IEEE Antennas Propag. Magazine*, Vol. 40, No. 2, 15–28, Apr. 1998.
4. Cocheril, Y. and R. Vauzelle, "A new ray-tracing based wave propagation model including rough surfaces scattering," *Progress In Electromagnetics Research*, PIER 75, 357–381, 2007.
5. Fuschini, F., H. El-Sallabi, V. Degli-Esposti, L. Vuokko, D. Guiducci, and P. Vainikainen, "Analysis of multipath propagation in urban environment through multidimensional measurements and advanced ray tracing simulation," *IEEE Trans. Antennas Propag.*, Vol. 56, No. 3, 848–857, Mar. 2008.
6. Alvar, N. S., A. Ghorbani, and H. R. Amindavar, "A novel hybrid approach to ray tracing acceleration based on pre-processing and bounding volumes," *Progress In Electromagnetics Research*, PIER 82, 19–32, 2008.
7. Wang, F. J. and J.-S. Zhang, "Wideband cavity-backed patch antenna for PCS/IMT2000/2.4 GHz WLAN," *Progress In Electromagnetics Research*, PIER 74, 39–46, 2007.
8. Qin, W., "A novel patch antenna with a T-shaped parasitic strip for 2.4/5.8 GHz WLAN applications," *Journal of Electromagnetic Waves and Applications*, Vol. 21, No. 15, 2311–2320, 2007.
9. Liu, L., J. P. Xiong, Y. Z. Yin, and Y. L. Zhao, "A novel dual-F-shaped planar monopole antenna for ultrawideband commu-

nications," *Journal of Electromagnetic Waves and Applications*, Vol. 22, No. 8–9, 1106–1114, 2008.

10. El-Fishawy, N. A., M. Shokair, and W. Saad, "Proposed Mac protocol versus IEEE 802.15.3a for multimedia transmission over UWB networks," *Progress In Electromagnetics Research B*, Vol. 2, 189–206, 2008.
11. Li, Z., C.-X. Zhang, G.-M. Wang, and W.-R. Su, "Designs on CPW-FED aperture antenna for ultrawideband applications," *Progress In Electromagnetics Research C*, Vol. 2, 1–6, 2008.
12. Gao, G.-P., X.-X. Yang, and J.-S. Zhang, "A printed volcano smoke antenna for UWB and WLAN communications," *Progress In Electromagnetics Research Letters*, Vol. 4, 55–61, 2008.
13. Sobli, N. M. and H. E. Abd-El-Raouf, "Design of a compact printed band-notched antenna for ultrawideband communications," *Progress In Electromagnetics Research M*, Vol. 3, 57–78, 2008.
14. Han, T.-Y. and C.-Y.-D. Sim, "Reconfigurable monopolar circular patch antenna for wireless communication systems," *Journal of Electromagnetic Waves and Applications*, Vol. 22, No. 5/6, 635–642, 2007.
15. Ghassemi, N., J. Rashed-Mohassel, M. H. Neshati, S. Tavakoli, and M. Ghassemi, "A high gain dual stacked aperture coupled microstrip antenna for wideband applications," *Progress In Electromagnetics Research B*, Vol. 9, 127–135, 2008.
16. Mahmoudian, A. and K. Forooraghi, "A novel planar leaky wave antenna for wireless application," *Journal of Electromagnetic Waves and Applications*, Vol. 22, No. 2/3, 313–324, 2008.
17. Jolani, F., A. M. Dadgarpour, and H. R. Hassani, "Compact M-slot folded patch antenna for WLAN," *Progress In Electromagnetics Research Letters*, Vol. 3, 35–42, 2008.
18. Wang, H., C.-Z. Gu, M.-K. Mu, W.-Z. Cui, W. Ma, J. Huangfu, and L.-X. Ran, "Design of leakywave coaxial cable compatible for both 2G and 3G wireless communications," *Journal of Electromagnetic Waves and Applications*, Vol. 22, No. 5/6, 731–740, 2008.
19. Ren, W., "Compact dual-band slot antenna for 2.4/5 GHz WLAN applications," *Progress In Electromagnetics Research B*, Vol. 8, 319–327, 2008.
20. Molina-Garcia-Pardo, J.-M., J.-V. Rodriguez, and L. Juan-Llacer, "Underestimation of the RMS delay spread when using uniform tapped delay lines in wireless communications," *Journal*

of Electromagnetic Waves and Applications, Vol. 22, No. 5/6, 872–881, 2008.

21. Li, X., L. Yang, S.-X. Gong, and Y.-J. Yang, "Bidirectional high gain antenna for WLAN applications," *Progress In Electromagnetics Research Letters*, Vol. 6, 99–106, 2009.
22. Zelley, C. A. and C. C. Constantinou, "A three-dimensional parabolic equation applied to VHF/UHF propagation over irregular terrain," *IEEE Trans. Antennas Propag.*, Vol. 47, No. 10, 1586–1596, Oct. 1999.
23. Zaporozhets, A. A. and M. F. Levy, "Modeling of radiowave propagation in urban environment with parabolic equation method," *Electron. Lett.*, Vol. 32, No. 17, 1615–1616, 1996.
24. Janaswamy, R., "Path loss predictions in the presence of buildings on flat terrain: A 3-D vector parabolic equation approach," *IEEE Trans. Antennas Propag.*, Vol. 51, No. 8, 1716–1728, Aug. 2003.
25. Awadallah, R. S., J. Z. Gehman, J. R. Kuttler, and M. H. Newkirk, "Effects of lateral terrain variations on tropospheric radar propagation," *IEEE Trans. Antennas Propag.*, Vol. 53, No. 1, 420–434, Jan. 2005.
26. Sacks, Z. S., D. M. Kingsland, R. Lee, and J.-F. Lee, "A perfectly matched anisotropic absorber for use as an absorbing boundary condition," *IEEE Trans. Antennas Propag.*, Vol. 43, No. 12, 1460–1463, Dec. 1995.